Journal of Nuclear Materials 389 (2009) 62–67

Contents lists available at ScienceDirect

Journal of Nuclear Materials

journal homepage: www.elsevier.com/locate/jnucmat

Monitoring the embrittlement of reactor pressure vessel steels by using the Seebeck coefficient

M. Niffenegger *, H.J. Leber

Paul Scherrer Institut, Nuclear Energy and Safety Department, Structural Integrity Group, 5232 Villigen PSI, Switzerland

ARTICLE INFO

PACS:
61.80.Hg
61.82.Bg
62.20.Mk

ABSTRACT

The degree of embrittlement of the reactor pressure vessel (RPV) limits the lifetime of nuclear power plants. Therefore, neutron irradiation-induced embrittlement of RPV steels demands accurate monitoring. Current federal legislation requires a surveillance program in which specimens are placed inside the RPV for several years before their fracture toughness is determined by destructive Charpy impact testing. Measuring the changes in the thermoelectric properties of the material due to irradiation, is an alternative and non-destructive method for the diagnostics of material embrittlement. In this paper, the measurement of the Seebeck coefficient ($\bar{K}$) of several Charpy specimens, made from two different grades of 22 NiMoCr 37 low-alloy steels, irradiated by neutrons with energies greater than 1 MeV, and fluencies ranging from 0 up to 4.5×10^{19} neutrons per cm^2, are presented. Within this range, it was observed that $\bar{K}$ increased by $\approx$500 nV/°C and a linear dependency was noted between $\bar{K}$ and the temperature shift $\Delta T_{41\,\mathrm{J}}$ of the Charpy energy vs. temperature curve, which is a measure for the embrittlement. We conclude that the change of the Seebeck coefficient has the potential for non-destructive monitoring of the neutron embrittlement of RPV steels if very precise measurements of the Seebeck coefficient are possible.

1. Introduction

During the operation of a nuclear power plant (NPP) several safety relevant reactor components may undergo loads leading to degradation of the structural material. Important degradation phenomena are thermo-mechanical fatigue due to varying temperature and mechanical load and the embrittlement of the reactor pressure vessel (RPV) due to neutron irradiation. The importance of these topics is revived by the current desire for lifetime extension of nuclear power plants. In order to guarantee safe operation, monitoring of such degradations is highly desirable. The RPV made from low-alloy ferritic (LAS) steel is one of the most important safety barriers between core and the environment of a nuclear reactor, therefore its integrity is of utmost importance. In this paper, we concentrate on the embrittlement of the RPV, especially on its determination by a non-destructive method called the thermoelectric power method (TEP).

1.1. Embrittlement of the reactor pressure vessel (RPV) due to neutron irradiation

Irradiation of RPV steels with a neutron fluence $\varphi \geqslant 10^{17}$ n/cm^2 and energies above 1 MeV may result in lattice defects, which are the origin for an increase of the yield strength and a decrease of fracture toughness (embrittlement). Influencing parameters for this effect are, e.g., the chemical composition, operating temperature, segregations of Cu and P, grain size, fluence and energy spectrum of the neutrons and the operation temperature.

Brittle behaviour is characterized by an abruptly cracking without preceding plastic deformation, whereas ductile material shows plastic deformation before failure. The brittleness and ductility are also functions of the temperature. Some materials show a distinct change of the ductility within a certain temperature range, the so-called ductile-to-brittle (DBT) transition zone. A measure for these properties is the energy needed to crack special V-notched specimens by beating them with a pendulum hammer. This fracture energy is also called Charpy energy corresponding to the inventor of this testing method. Since a brittle failure of the RPV would result in a catastrophic accident, the lifetime of a NPP is limited by the achievement of the minimal allowed fracture toughness.

In the mandatory national surveillance program, Charpy V-notched specimens made from original RPV steel are irradiated in a NPP followed by Charpy impact testing. The fracture energy is measured as a function of the temperature, yielding a Charpy energy vs. temperature curve. Material embrittlement due to neutron irradiation can be characterized by the temperature shift $\Delta T_{41\,\mathrm{J}}$ of the DBT-zone, as shown in Fig. 1. The index 41 J indicates that the temperature shift of the DBT-zone is measured at the energy of 41 J.

* Corresponding author. Tel.: +41 56 310 2686; fax: +41 56 310 2199.
E-mail address: Markus.Niffenegger@psi.ch (M. Niffenegger).
URL: http://www.psi.ch (M. Niffenegger).

0022-3115/$ - see front matter © 2009 Elsevier B.V. All rights reserved.
doi:10.1016/j.jnucmat.2009.01.008

Beside the embrittlement, neutron irradiation leads to changes of several material properties. These changes can be used as indicators for the state of the degradation, i.e., the decrease of fracture toughness. One physical effect that might be used for the detection of material degradation is the Seebeck effect. It is one of several thermoelectric effects, mainly used for measuring temperatures with thermocouples [1]. Thomas Seebeck discovered in 1821 that a heat flow is accompanied with a small electric current. Within a certain temperature range, the generated electric field is proportional to the temperature gradient whereby the proportionality factor is called Seebeck coefficient ($\bar{K}$). We shall summarize the main equations coming from the theory of thermoelectricity, which are essential to understand the origin of the thermoelectric power and to interpret the measured results. A more detailed derivation of the theory of thermoelectricity based on quantum mechanics is given in Ref. [2].

Neutron irradiation, heat treatments and plastic material deformations are leading to a drift of the $\bar{K}$ [3–6]. However, if the change of $\bar{K}$ is a well-defined function of the neutron fluence and if the effect is large enough compared with that of other influencing parameters, it could be used for monitoring of material embrittlement, which in the case of the RPV is correlated to the neutron fluence. The application of the $\bar{K}$ for measuring the embrittlement has been investigated in the past decade by a small community. Some investigations of the TEP-method were performed within the framework of the European network Ageing Materials Evaluation and Studies (AMES) by Electricité de France (EDF) [7] and Joint Research Centre (JRC) in Petten [8]. At the Paul Scherrer Institut (PSI) the application of the TEP-method for material diagnostic is under investigation since 2001 [9]. At PSI measurements were performed on both, irradiated and fatigued specimens by using a TEP-device developed by the Institut National des Sciences Appliquées de Lyon (INSA).

In this paper, we present the $\bar{K}$ of two investigated LAS RPV steels of the type 22 NiMoCr 37 corresponding to ASTM 533-B Cl.1 and ASTM 508 Cl. 2, respectively. One grade is the well characterized Japanese RPV-reference material JRQ [10] made by Kawasaki Steel Corporation at Mizushima Works, whereas the second grade stems from a Swiss nuclear power plant. The chemical compositions of the two materials are given in Tables 1a and 1b, respectively. Charpy specimens were made from both materials. The specimens made from JRQ-steel were irradiated at the PSI research reactor Saphir, whereas the second set of samples stem from the surveillance program and were therefore irradiated in a NPP.

We further compare the measured Seebeck coefficients with those measured on Charpy samples made from un-irradiated Incoloy 800. This comparison shall support the thesis, that the scatter of $\bar{K}$, which was observed for the RPV material, can be explained by inhomogeneous material properties and by the inherent uncertainties in the DBT-zone. Technical reasons (small gauge volume) of the measuring method may be an additional origin for the scatter of $\bar{K}$.

2. The Seebeck effect and its measurement

In solids, the heat is transported by phonons and by free electrons. For metals, the main contribution to the heat transport stems from the electrons. Thus, electrons are carriers of both, thermal energy and electric charge. That means: thermal and electric currents are coupled phenomena with the consequence, that an electric current accompanies a heat flow. This is the origin of the Seebeck effect whose manifestation is a thermoelectric voltage, in the following called thermoelectric power. In this paragraph we only emphasize the relevant results of the theory of thermoelectricity, some of its practical aspects and interpretations.

The important results of the thermoelectric theory are the two coupled Eqs. (1) and (2) for the electrical j_E and thermal current j_Q as a function of their origins, electric field E_x and temperature gradient dT/dx. The suffix x indicates that we only consider the x-direction

$$j_E = L^{11}E_x + L^{12}\left(\frac{-dT}{dx}\right), \tag{1}$$

$$j_Q = L^{21}E_x + L^{22}\left(\frac{-dT}{dx}\right). \tag{2}$$

In the above equations, the so-called transport coefficient L^{12} expresses that a temperature gradient is associated with an electrical current, whereas L^{21} represent the heat flow as a consequence of an electrical field. L^{11} and L^{22} are the electrical and heat conductivity, respectively. Eqs. (1) and (2) describe both, the Seebeck and its inversion, the Peltier effect. With the assumption $j_E = 0$, i.e., if we measure the electric potential using a high resistance voltmeter, we get from Eq. (1) the electric field inside the metal:

$$E_x = \left(L^{11}\right)^{-1}(L^{12})\frac{\partial T}{\partial x} = K(T)\frac{\partial T}{\partial x}. \tag{3}$$

The appearance of an electric field as a consequence of a temperature gradient is known as the Seebeck effect. For an applied electric field and a vanishing temperature gradient we get from Eqs. (1) and (2) the equations for the thermal and electrical current:

$$j_Q = L^{21}E_x \quad \text{and} \quad j_E = L^{11}E_x, \tag{4}$$

that can be summarized to

$$j_Q = L^{21}(L^{11})^{-1}j_E \quad \text{or} \quad j_E = L^{11}(L^{21})^{-1}j_Q, \tag{5}$$

where the coefficient $L^{21}(L^{11})^{-1}$ is the so-called Peltier coefficient. The thermoelectrical potential difference U (called thermoelectric voltage or thermoelectric power) between two points 0 and 1 of a specimen is the line integral of E_x evaluated from point 0 to 1

Table 1a
Chemical composition of JRQ-steel in wt%.

C	Si	Mn	P	S	Mo	Ni	Cr	Cu	V	Co	Al
0.19	0.25	1.39	0.019	0.0040	0.50	0.83	0.12	0.140	0.003	0.000	0.012

Table 1b
Chemical composition of 22 NiMoCr 37-steel from NPP in wt%.

C	Si	Mn	P	S	Mo	Ni	Cr	Cu	V	Co	Al
0.18	0.15	0.82	0.005	0.008	0.54	0.96	0.39	0.08	<0.01	0.014	0.016

$$U = \int_0^1 E_x(x)dx = \int_0^1 dxK(T,x)\frac{\partial T}{\partial x} = \int_{T_0}^{T_1} K(T,x)dT = \bar{K}(T_1 - T_0), \tag{6}$$

where the mean Seebeck coefficient $\bar{K}$ is

$$\bar{K} = \frac{1}{(T_1 - T_0)}\int_{T_0}^{T_1} K(T,x)dT, \tag{7}$$

or because the temperature T is a function of the space coordinate x

$$\bar{K} = \frac{1}{(T_1 - T_0)}\int_0^1 K(T,x)\frac{\partial T}{\partial x}dx = \frac{U}{(T_1 - T_0)}. \tag{8}$$

Eq. (6) expresses that the thermoelectric voltage U, which is generated between two points, is proportional to the temperature difference between these points whereas the proportionality factor is the mean Seebeck coefficient $\bar{K}$. However, it is essential to realize that the thermoelectric voltage is generated only in the area with a non-vanishing temperature gradient. Furthermore, if the two points are at the same temperature ($T_0 = T_1$) as in a closed loop, the integral (6) is zero in a homogeneous ($K(x)$ = constant) material. However, in an inhomogeneous material, where $K(x)$ is an explicit function of the x-coordinate, we will get a thermoelectric voltage U, even if $T_0 = T_1$ and the temperature on the integration path is not constant. Based on these properties of Eq. (6) we can determine $\bar{K}$ from a measurement of the thermoelectric voltage U while applying a temperature difference $(T_1 - T_0)$ on a specimen.

According to Eqs. (3) and (6) $\bar{K}$ is a function of the transport coefficients which depend on the scattering of electrons on lattice defects. This means that $\bar{K}$ will change if the amount of lattice defects is increased or decreased and the mean Seebeck coefficient $\bar{K} = U/(T_1 - T_0)$ can therefore be used to characterize the change of the mean material properties, e.g., embrittlement of the material due to neutron irradiation.

Furthermore, if we scan the specimen by moving a local temperature gradient along the specimen's surface, we can detect also localized inhomogeneities in the material by measuring U according to Eq. (6).

2.1. Experimental setup for measuring the thermoelectric power

For measuring the Seebeck coefficient ($\bar{K}$) of Charpy specimens we used a TEP-device developed by INSA de LYON. The instrumentation consists of two parts. One part is used to apply the temperature gradient on the specimen and to measure both, temperatures and thermoelectric power. In order to measure radio-active specimens this device can be operated in hot cells. The second part of the equipment processes the data acquired by the transducer. It is an easy to use control instrument which can be operated via touch screen or an external PC and is placed outside the hot cell. The specimens can be fixed by pressing them with a pneumatic piston on two supports made of copper, whereas the pressure is held constant in order to guarantee well-defined contacts between sample and the supports. These contacts are held on two different temperatures fixed at 15 ± 0.1 °C and 25 ± 0.1 °C, respectively. The two temperatures are measured by thermocouples which are located near the contact surface of the support. The test temperatures are controlled by internal Peltier elements, cooling water, platinum resistance sensors and resistant heating. After stabilizing the system, the thermoelectric power and the temperatures are measured and the resulting Seebeck coefficient is calculated. The amplifier for the thermoelectric voltage has a resolution of 5 nV and an excellent stability due to temperature changes. To avoid drift of the measured values caused by the electronic device, periodically calibrations by using a reference material are performed.

Special attention has to be paid on the cleanness of the surface where the electrodes are in touch with the specimen, since an oxide layer or any pollution leads to unreliable results. An indicator for an insufficiently clean surface is the drift of the $\bar{K}$ signal that results in a long time to achieve stability of the output signal. Surface effects are the reason for one part of the scatter band in the presented results. Therefore, the oxide layer was removed by mechanically grinding and polishing the surface.

3. The change of Seebeck coefficient due to neutron irradiation of JRQ-steel

3.1. Neutron irradiation history

Irradiation was performed at a neutron flux of $\approx 5 \times 10^{12}$ n/cm^2 (>1 MeV) and a temperature of 290 °C in the 10 MW SAPHIRE reactor of PSI. One set (I) of specimens was irradiated with four fluencies ranging from zero up to 0.39–5 $\times 10^{19}$ n/cm^2. An additional set (IAR) was irradiated up to $\varphi = 2.5 \times 10^{19}$ n/cm^2, then annealed (18 h at 460 °C) before re-irradiated up to 4.51 $\times 10^{19}$ n/cm^2.

The Charpy impact testing was performed at Oak Ridge National Laboratory (ORNL) and described in [11,12]. Fig. 1 shows the Charpy energy vs. temperature for the un-irradiated, the irradiated (I) and the irradiated-annealed and re-irradiated (IAR) JRQ material. In Fig. 2 the shift ΔT_{41J} is given as a function of the fluence. A shift $\Delta T_{41\ J}$ of about 95 °C was observed for the I-material which was irradiated with a fluence of 5 $\times 10^{19}$ n/cm^2. For the IAR-material this shift is 65 °C.

Fig. 3 shows the obtained Seebeck coefficients vs. neutron fluence for the I- and IAR-specimens, respectively. It appeared a clear correlation between the Seebeck coefficient and fluence. With increasing fluence the $\bar{K}$ rises in a similar monotonic slope for both, the I- and the IAR-specimens. However, a pronounced offset between the two slopes is observed. This offset, which is also observed in Fig. 1, is supposed to be an effect of the annealing.

3.2. Correlation of the Seebeck coefficient with neutron embrittlement

By comparing the ΔT_{41J} vs. the fluence (Fig. 2) with $\bar{K}$ vs. the fluence (Fig. 3), we recognize a similar slope. This suggests to draw ΔT_{41J} as a function of $\bar{K}$. As shown in Fig. 4, we obtained an almost linear relation between $\bar{K}$ and ΔT_{41J} with a steeper slope of the I-specimens (7 nV/°C) than for the IAR-specimens (10 nV/°C). This linear correlation is useful, because once known, it could be used

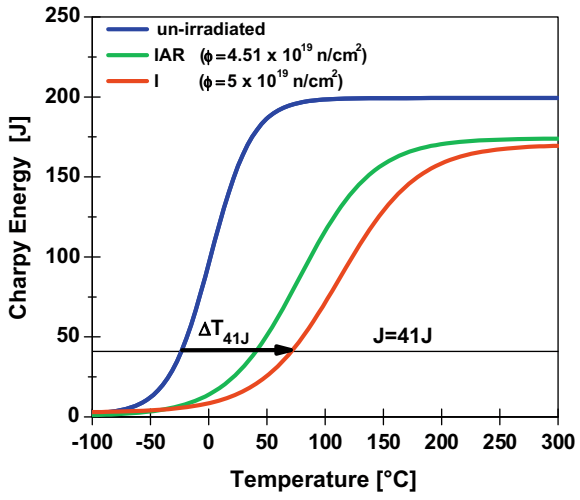

Fig. 1. Charpy energy vs. temperature for un-irradiated ($\varphi = 0$ n/cm^2), irradiated (I) and irradiated-annealed-re-irradiated (IAR) specimens [2].

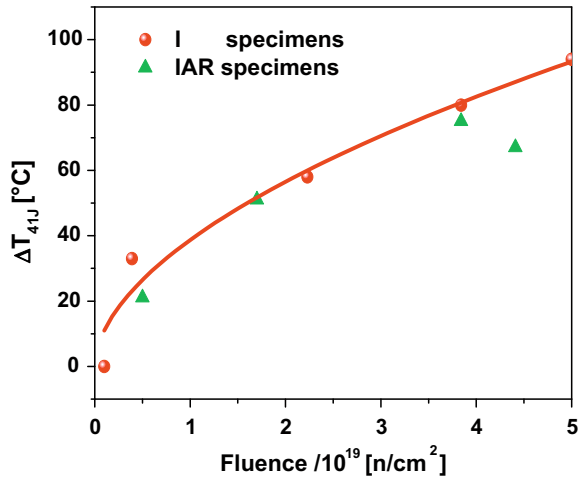

Fig. 2. Shift ΔT_{41J} of the transition temperature vs. the fluence for the I- and IAR-specimens.

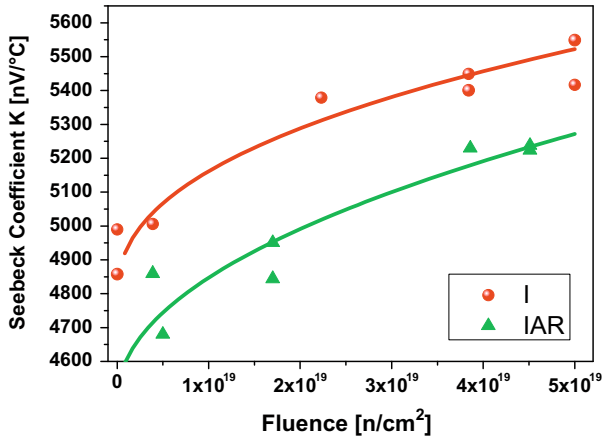

Fig. 3. Seebeck coefficient measured on irradiated (I) and irradiated, annealed and re-irradiated (IAR) specimens.

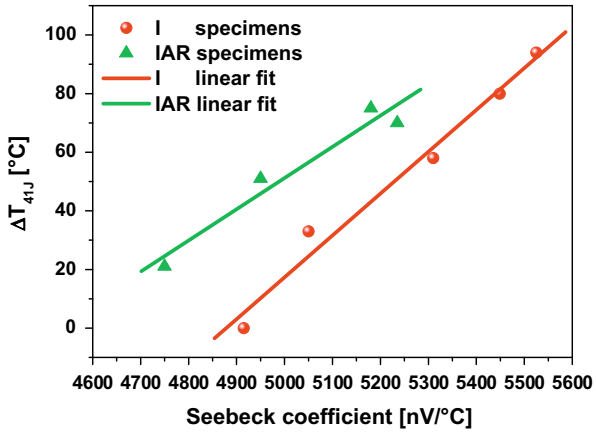

Fig. 4. Correlation between ΔT_{41J} and Seebeck coefficient for the I- and IAR-specimens.

for monitoring the neutron embrittlement by just measuring $\bar{K}$. However, even a clear monotonic change of $\bar{K}$ vs. the fluence is observed, its magnitude is very small and therefore precise measurements are essential.

4. The Seebeck coefficient of surveillance specimens

Un-irradiated and irradiated Charpy specimens from the surveillance program of a NPP were extensively analysed by measuring the Seebeck coefficient. The Charpy V-notched specimens made from steel 22 NiMoCr 37 were irradiated in the RPV of a pressurized water reactor (PWR) at a temperature of 300 °C with fluencies ranging from 0 up to 2.6×10^{19} n/cm^2. Note that the specimens stem from the base material of the upper shell ring of the RPV and were placed near the core were they accumulated a much higher fluence than the inner wall of the RPV, which is yielded by a water gap. The chemical components of 22 NiMoCr 37 are given in Table 1b.

Fig. 5 shows the increase of $\bar{K}$ vs. the fluence. A monotonic increase of $\bar{K}$ vs. the fluence is observed. For this material an increase of about 300 nV/°C corresponds for this material to a shift in the transition temperature ΔT_{68} of 30 °C. Note that the plotted values are mean values, each resulting from a couple of specimens and therefore characterized with a standard deviation of up to about 70 nV/°C which is also given in the graph. The mean values of $\bar{K}$, its standard deviation (STD) and the error are given in the legend. Note that, since the results stem from a few specimens, the resulting STD is relatively large. Further reasons for the large scatter are discussed in the next paragraph.

4.1. Accuracy of the TEP-method

As shown in the presented results, the scatter of $\bar{K}$ is rather large. However, several reasons for the scatter of the Seebeck coefficient which may explain at least one part of the scatter of $\bar{K}$ were found:

- The Charpy energy, determined by classical destructive testing, shows large scatter, especially in the ductile-to-brittle transition zone. A large scatter of the Charpy energy in the dBT-zone is characteristic for the DBT-zone of RPV steels. For the JRQ material more detailed information concerning the fracture toughness can be found in [3].
- The manufacturing process may induce anisotropic material properties and therefore $\bar{K}$ depends on the orientation of the Charpy specimen relative to the feedstock.
- Also the position of the specimens on the cooper holder was detected as a source of the scatter of $\bar{K}$. The reason for this may lie in local inhomogeneties which can influence the measure if taken from a small gauge volume as it is the case in the described TEP-method.

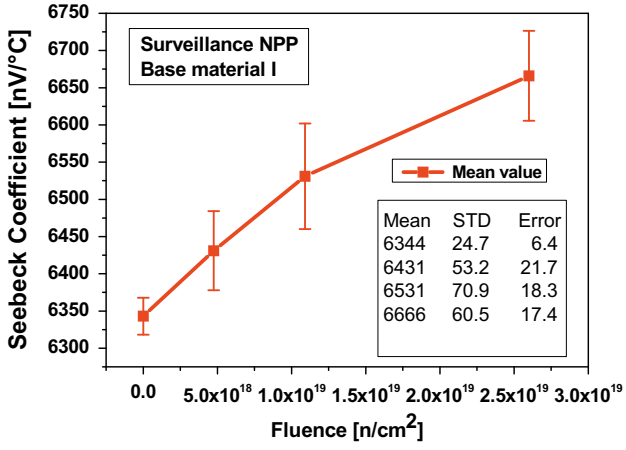

Fig. 5. Seebeck coefficient of irradiated surveillance specimens vs. fluence.

• An other source of the scatter is spatial variations of the material properties which appear in large components. This was confirmed by measuring two sets of JRQ-specimens taken from two different depths (45 and 136 mm) of a block having a thickness of 225 mm. A difference of $\bar{K}$ between the two sets of about 100 nV/°C was revealed.

4.2. Comparison with un-irradiated Charpy specimens (Incoloy 800)

As shown before, the Seebeck coefficient of RPV material shows a rather large scatter which partially can be explained by material inhomogeneities. In order to demonstrate that the reason for the scatter does not lie in the electronic of the measuring device, a set of specimens made from Incoloy 800 were measured. Incoloy 800 with its austenitic matrix does not show a steep change of the fracture toughness within a DBT-zone as the ferritic RPV steels do and therefore a smaller scatter of the fracture toughness can be expected. Furthermore, this material is expected to be more homogeneous than the JRQ material. For this material indeed very good reproducibility and small scatter of the Seebeck coefficient has been observed. The mean $\bar{K}$ of 136 specimens is −2779 nV/°C with a standard deviation of 16 nV/°C.

5. Microstructure of steel ASTM 533-B Cl.1 and Incoloy 800

The microstructural examination of the heat treated JRQ-steel revealed anisotropy at the macroscopic level. Fig. 6 shows elongated dark streaks. Since the latter are visible on both sections of the specimen, they must have a flaky three-dimensional shape and are parallel to the plate faces. The appearance of streaks is a consequence of the (continuous) casting and hot rolling process of the metal plate. They represent regions in which solidification of the steel took place at last. Therefore, these regions contain portions of elements which are not able to be in solid solution in the metallic crystal. In these streaks most of non-metallic inclusions like oxides and manganese sulphides are observed. As the streaks have a larger average dimensions on the longitudinal (parallel to the rolling direction) section than on the transversal (perpendicular to the rolling direction), it can be concluded that the dark flake shaped regions were elongated by the rolling process of the plate. At a closer view it is revealed that the dark regions consist of dense fine globular carbides in a distorted ferrite matrix, whereas the brighter regions are composed of coarser granular carbides in the same ferrite matrix. It is expected that the resulting heterogeneity combined with the observed anisotropy of the streaks affects the reproducibility of the TEP measurements depending on the orientation of the Charpy specimens in the plate.

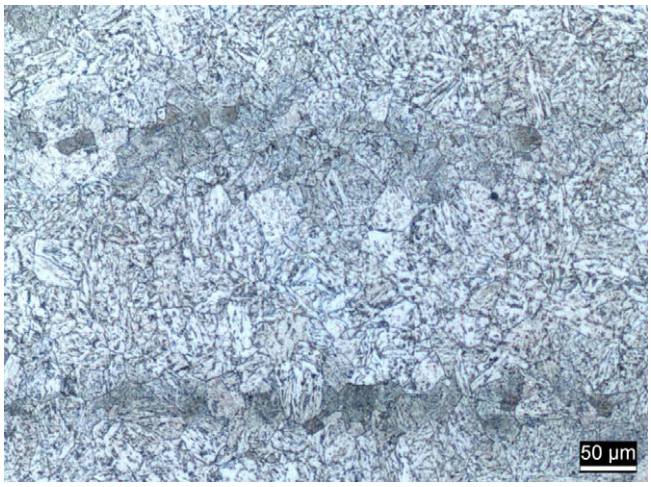

Fig. 6. Micrograph of Charpy V notch specimen of heat treated thick plate JRQ: longitudinal section, parallel to the rolling direction showing the transition from dark streak (top) with mainly globular carbides to brighter matrix (bottom) with granular carbides in distorted ferrite.

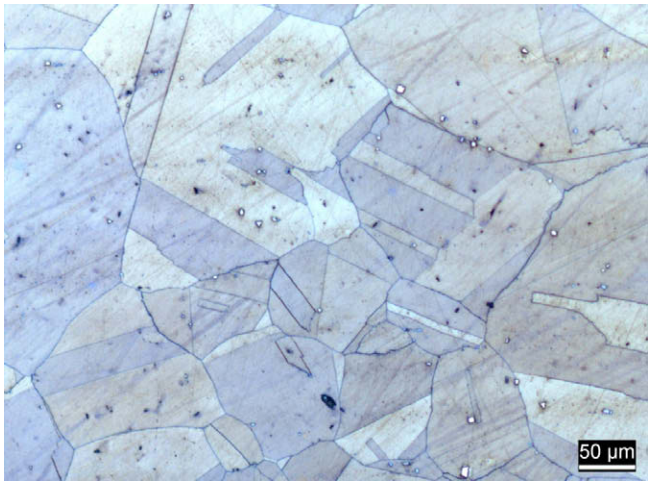

Fig. 7. Micrograph of Charpy V notch specimen of Incoloy 800 showing the homogeneous austenite matrix.

Unlike the JRQ material, the microstructure of the Incoloy 800 possesses a more homogeneous appearance. Fig. 7 shows the matrix that consists of austenite, a solid solution of the base element and of most alloying metallic elements.

6. Conclusions

The embrittlement of Charpy specimens, made from two different steel products of type 22 NiMoCr 37, irradiated by neutrons with energies greater than 1 MeV, was determined. The corresponding Seebeck ($\bar{K}$) coefficients were measured. Within the fluence rang from 0 up to 4.5×10^{19} neutrons per cm^2, it was observed that $\bar{K}$ monotonically increased by ≈500 nV/°C. Furthermore a linear dependency between $\bar{K}$ and the temperature shift $\Delta T_{41\,J}$ of the Charpy energy vs. temperature curve, which is a measure for the material embrittlement, was noted. However, the inhomogeneity of RPV material may lead to large scatter of $\bar{K}$. For comparison, an additional material, namely Incoloy 800 was analysed. Since this material does not show a pronounced change from brittle to ductile behavior, a much smaller scatter of the fracture toughness can be expected than for 22 NiMoCr 37. Furthermore, Incoloy 800 is more homogeneous than the RPV material as shown by metallography. Indeed, much smaller scatter and a very good reproducibility of $\bar{K}$ was obtained for Incoloy 800. We therefore conclude that the reason for one part of the scatter lies in the inhomogeneity of the material combined with the applied measuring method in which the measured properties stem from a very small volume near the heat source/sink [9] which is needed to apply the temperature gradient on the specimen's surface. To avoid such problems, i.e., to improve the quality of the TEP measurements, we propose to modify the measuring technique in order to achieve a larger gauge volume that allows averaging of the inhomogeneity so that the measured values reflect bulk properties which are more representative for the material state. However, some inherent scatter of the fracture toughness and therefore of $\bar{K}$ in the DBT-zone will remain.

For the application of the reported method, it seems realistic to measure $\bar{K}$ of the surveillance specimens after certain fluence and mounting them again inside the RPV for further irradiation. Such a

non-destructive testing method would save a number of surviillance specimens and would allow a screening of the neutron-induced embrittlement of RPV in nuclear power plants.

Acknowledgments

The financial support for this work by the Swiss Federal Nuclear Inspectorate (HSK) is gratefully acknowledged. We thank our colleagues M. Suter, P. Simon and U. Tschanz for the sample preparation and their help in measuring the Seebeck coefficient.

References

[1] A.W. Fenton, Nucl. Eng. 19 (1) (1980) 61.
[2] H. Ibach, H. Lüth, Solid-State Physics, Springer-Verlag, 1995.
[3] D.G. Sanders, ISA Trans. 13 (1974) 200–211.
[4] V.A. Krivtsov, Teploenergetika 20 (10) (1973) 73.
[5] D.R. Keyser, Instrum. Control Syst. 47 (3) (1974) 51.
[6] T.G. Kollie et al., Rev. Sci. Instrum. 46 (11) (1975).
[7] J.F. Coste, J.M. Leborgne, J.P. Massoud, O. Grisot, S. Miloudi, R. Borrelly, Application of Thermoelectricity to NDE of Thermally Aged Cast Duplex Stainless Steels and Neutron Irradiated Ferritic Steels, EPRI Workshop and NDE for Damage Assessment, La Jolla, 6–7 October 1997.
[8] L. Debarberis, B. Acosta, et al., Assessment of steels ageing by measuring the Seebeck and Thomson effects (STEAM), in: Proceedings of the 15th World Conference on Non-destructive Testing, in Rome, 15–21 October 2000.
[9] M. Niffenegger, K. Reichlin, D. Kalkhof, Nucl. Eng. Des. 235 (2005) 1777.
[10] F. Gillemot, E. Czoboly, G. Uri, Final Database Report on IAEA CRP on Optimizing of Reactor Pressure Vessel Surveillance Programmes and their Analyses, vol. 2, IWG-LMNPP-94/7, Produced by IAEA, 1994.
[11] R.K. Nanstad et al., Irradiation and post-annealing reirradiation effects on fracture toughness of RPV steel heat JRQ, the effects of radiation on materials, in: M.L. Grossbeck (Ed.), Proceedings of the 21st International Symposium, ASTM STP 1447, ASTM International, West Conshohocken, PA, 2004.
[12] R.K. Nanstad et al., J. ASTM Int. 2 (9) (2005). Paper ID JAI12888.